

Short note

## Shape co-existence and structural evolution of the yrast band in $^{157}\text{Yb}$

Y. Zheng<sup>1,a</sup>, X.H. Zhou<sup>1</sup>, Y.H. Zhang<sup>1</sup>, Y.X. Guo<sup>1</sup>, X.G. Lei<sup>1</sup>, Z. Liu<sup>1</sup>, J.J. He<sup>1</sup>, M.L. Liu<sup>1</sup>, W.J. Luo<sup>1</sup>, S.X. Wen<sup>2</sup>, L.H. Zhu<sup>2</sup>, and C.X. Yang<sup>2</sup>

<sup>1</sup> Institute of Modern Physics, Chinese Academy of Sciences, Lanzhou 730000, PRC

<sup>2</sup> China Institute of Atomic Energy, Beijing 102413, PRC

Received: 7 January 2002 / Revised version: 10 April 2002  
Communicated by D. Schwalm

**Abstract.** The high-spin states of  $^{157}\text{Yb}$  have been studied via the  $^{144}\text{Sm}(^{16}\text{O}, 3n)$  reaction at  $^{16}\text{O}$  energy of 90 MeV using techniques of in-beam  $\gamma$ -ray spectroscopy. Measurement of  $\gamma$ - $\gamma$ - $t$  coincidences was performed with 11 BGO(AC)HPGe detectors. Based on the measured results of  $\gamma$ - $\gamma$  coincidences,  $\gamma$ -ray anisotropies and DCO ratios, the level scheme for  $^{157}\text{Yb}$  was established. The shape co-existence and structural evolution of the  $\nu i_{13/2}$  band with increasing angular momentum in  $^{157}\text{Yb}$  have been discussed. The systematics of the  $\nu i_{13/2}$  bands in the  $N = 87$  odd- $A$  isotones have been compared.

**PACS.** 23.20.Lv Gamma transitions and level energies – 27.70.+q  $150 \leq A \leq 189$

In the rare-earth region, the so-called transitional nuclei with  $N = 87$  are located at the border line between two groups of nuclei, with characteristics of single-particle excitations and collective rotational excitations, respectively. For the  $N < 87$  nuclei, the excited states consist mainly of proton and neutron quasiparticles coupled to large angular momenta [1–3]. In contrast, the nuclei with  $N > 87$  display a rotational decay pattern at low and moderately high spins which seems to terminate while the nucleus develops an oblate shape at higher spins [3–6]. Thus, the rare-earth nuclei with  $N = 87$  should manifest the pronounced transitional behavior, that is, both single-particle and rotational degrees of freedom co-exist and generate angular momentum in the same nucleus [7–9]. Moreover, the theoretical calculations indicate that the nuclei with  $N = 87$  should experience a special shape transition along the yrast line from prolate through soft-triaxial to oblate, the so-called band termination [8, 9]. In such a case, a nucleus undergoes a gradually loss of collectivity while the nuclear shape acquires an axial symmetry with respect to the direction of the spin due to the alignment of high- $j$  quasiparticles. Therefore, the  $N = 87$  nuclei are expected to provide a best environment to study the shape co-existence and shape transition effects through the interplay of individual and collective degrees of freedom. So far, high-spin states have been reported in three  $N = 87$  odd- $A$  nuclei with  $Z > 64$  [7–11]. Among these nuclei,

the yrast excitations in  $^{153}\text{Dy}$  and  $^{155}\text{Er}$  are built on the  $\nu i_{13/2}$  orbit and have energy spacings which follow the  $E \sim I(I + 1)$  rotational law [7–10], while the yrast level sequence in  $^{159}\text{Hf}$  is based on the  $\nu h_{9/2}$  configuration and has vibration-like spacings [11]. It would be of interest to find the yrast excitations in  $^{157}\text{Yb}$  and to study the structural change along the yrast line in the  $N = 87$  odd- $A$  isotone chain.

Before the present study, the  $13/2^+$  isomer with a quite pure  $\nu i_{13/2}$  configuration and several low-lying levels have been reported in  $^{157}\text{Yb}$  [12–14], but a high-spin level scheme has not yet been published. Here, we report on a level scheme for  $^{157}\text{Yb}$  up to an excitation energy of about 5.3 MeV.

The excited states in  $^{157}\text{Yb}$  were populated via the  $^{144}\text{Sm}(^{16}\text{O}, 3n)^{157}\text{Yb}$  reaction. The  $^{16}\text{O}$  beam was produced by the tandem accelerator at the China Institute of Atomic Energy (CIAE). The target was an isotopically enriched  $^{144}\text{Sm}$  metallic foil of 1.3 mg/cm<sup>2</sup> thickness with a 7 mg/cm<sup>2</sup> Pb backing. This combination of projectile and target was used previously, and the beam energy of 88 MeV was chosen to be suitable for populating high-spin states in  $^{157}\text{Yb}$  [14]. In the present work,  $\gamma$ - $\gamma$ - $t$  coincidence measurements were performed at a beam energy of 90 MeV with 11 BGO(AC)HPGe detectors, having energy resolutions of 1.9–2.3 keV at 1.33 MeV. Here,  $t$  refers to the relative time difference between any two coincident  $\gamma$ -rays detected within  $\pm 200$  ns. These detectors were

<sup>a</sup> e-mail: zhengyong@impcas.ac.cn

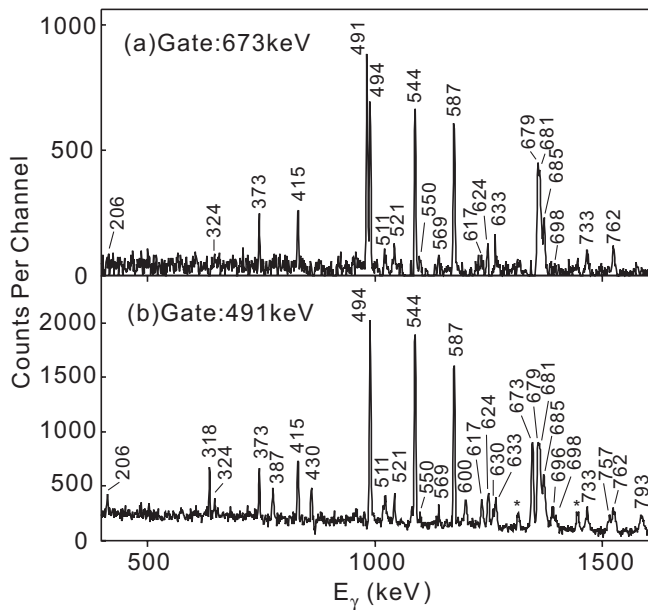


**Fig. 1.** Spectra of  $\gamma$ -rays gated on the 673 and 491 keV transitions, respectively. The \* symbols indicate contaminations.

divided into 3 groups positioned at  $35^\circ$  ( $145^\circ$ ),  $55^\circ$  ( $125^\circ$ ), and  $90^\circ$  with respect to the beam direction, so that the DCO ratios (directional correlations of  $\gamma$ -rays de-exciting the oriented states) could be deduced. All detectors were calibrated using the standard  $^{152}\text{Eu}$  and  $^{133}\text{Ba}$  sources. A total of  $120 \times 10^6$  coincidence events were accumulated. After accurate gain matching, these coincidence events were sorted out into a symmetric total matrix and an asymmetric DCO matrix for off-line analysis. Additionally, in order to extract information concerning  $\gamma$ -ray anisotropies, the coincidence data were sorted out into two asymmetric matrices whose  $x$ -axes were the  $\gamma$ -ray energy deposited in the detectors at any angles and  $y$ -axes were the  $\gamma$ -ray energy deposited in the detectors at  $35^\circ$  and  $90^\circ$ , respectively. By gating on the  $x$ -axis with suitable  $\gamma$ -rays, two spectra measured at  $35^\circ$  and  $90^\circ$  angle positions were obtained. After correcting for the overall detection efficiency of the detectors at each of the two angles and normalizing the two spectra with respect to each other,  $\gamma$ -ray anisotropy was deduced from the intensity ratio in the two spectra. Typical  $\gamma$ -ray anisotropies for the known  $\gamma$ -rays observed in this experiment were  $1.5(\pm 0.3)$  for stretched quadrupole transitions and  $0.7(\pm 0.2)$  for stretched pure dipole transitions. Therefore, we assigned the stretched quadrupole transition and stretched dipole transition to the  $\gamma$ -rays of  $^{157}\text{Yb}$  with anisotropies around 1.5 and 0.7, respectively. The reliability of the  $\gamma$ -ray anisotropy analysis was checked using the known  $\gamma$ -rays produced in the  $^{150}\text{Nd}(^{13}\text{C}, \alpha 3n)^{156}\text{Gd}$  reaction [15].

Assignments of the observed  $\gamma$ -rays to  $^{157}\text{Yb}$  were based on the coincidences with the known  $\gamma$ -rays [13,14]. Gated spectra were produced for each of the  $\gamma$ -rays assigned to  $^{157}\text{Yb}$ . Selected gated spectra are shown in fig. 1. Based on the analysis of the  $\gamma$ - $\gamma$  coincidence relationships, a level scheme for  $^{157}\text{Yb}$  is proposed, as shown in fig. 2.

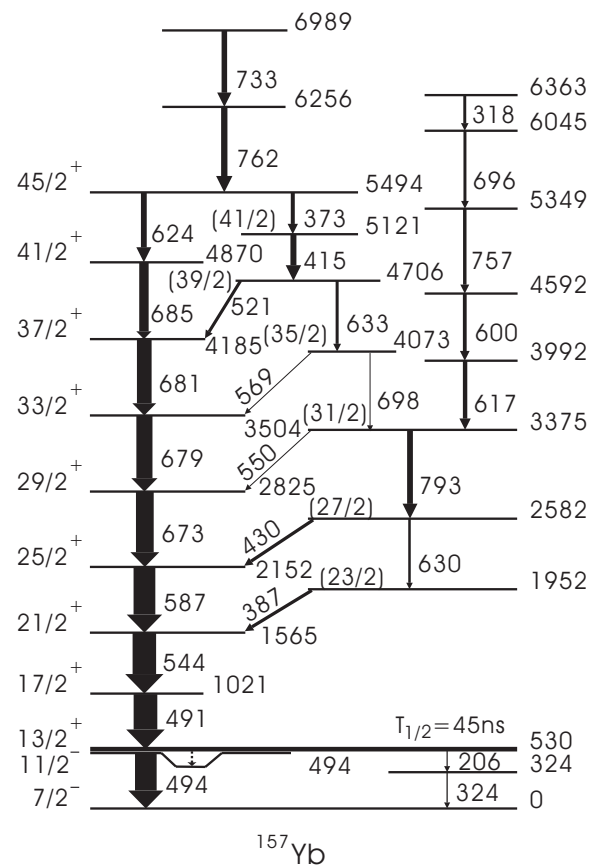


**Fig. 2.** Level scheme of  $^{157}\text{Yb}$  proposed in the present work.

The orderings of the transitions in the level scheme were fixed either with the help of some cross-over transitions or from the consideration of intensities in the gated spectra. The spins for the levels have been proposed according to the analysis of DCO ratios and  $\gamma$ -ray anisotropies. It is noted that a quite weak cascade of 206 and 324 keV transitions is in coincidence with all strong lines, excepting the 494 keV one. Although the 206 and 324 keV transitions are too weak to determine their transition orders, with the addition of these two transitions in the level scheme the energies of all levels are established firmly. Particularly, the excitation energy of the  $13/2^+$  isomer is fixed at 530 keV. This isomer was reported in the previous work [14], but its excitation energy remains unknown. The low-lying level structure of  $^{157}\text{Yb}$  resembles those of the lighter  $N = 87$  isotones [7–10]. In all of these isotones the  $13/2^+$  isomers were observed, and these isomers are depopulated by a low energy transition to a  $11/2^-$  state decaying to the  $\nu f_{7/2}$  ground state.

Above the  $13/2^+$  isomer, the level scheme of  $^{157}\text{Yb}$  is dominated by two parallel transition sequences. One of them, built on the  $13/2^+$  isomer and strongly populated, shows a rotation-like cascade of  $E2$  transitions at low spins, and then its structure changes into vibration-like excitations with five successive transitions having almost the same energies. Based on the systematics of the level structure in the  $N = 87$  isotones [7–10], this sequence of transitions should be the  $\nu i_{13/2}$  band, and it terminates at state

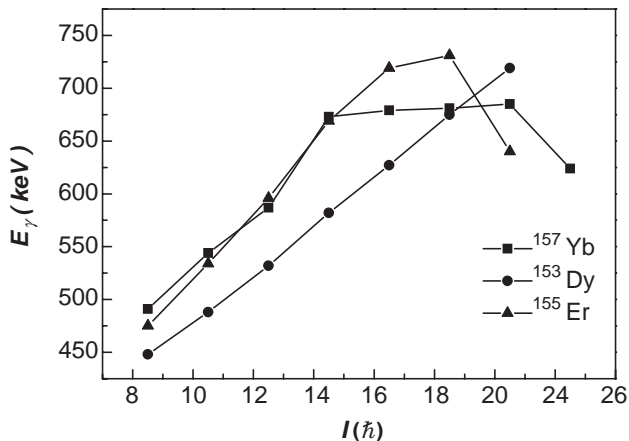


**Fig. 3.** Plots of  $E_\gamma$  vs.  $I$  for the  $\nu i_{13/2}$  band in  $^{153}\text{Dy}$ ,  $^{155}\text{Er}$  and  $^{157}\text{Yb}$ , respectively.

with spin value of  $45/2$ . The other one consists of irregular  $E2$  transitions and connects with the above-mentioned  $\nu i_{13/2}$  band by five dipole transitions. This irregular sequence is very similar to that in the neighboring isotope of  $^{155}\text{Er}$ , which has most likely the slightly oblate configuration of  $\nu [f_{7/2}^3 h_{9/2} i_{13/2}]$  [9]. The  $\nu i_{13/2}$  band exhibits collectivity at low spins in smoothly increasing transition energies, and loses its collectivity at high spins as manifested by the appearance of equidistant spaced levels. In the region around excitation energy of 5 MeV, where the band termination occurs, the level scheme shows several competing de-excitation pathways consisting of dipole and quadrupole transitions with irregular energies. These observations indicate that the low-spin collective character of  $^{157}\text{Yb}$  gives way to single-particle excitations at high spins. This structural phenomenon is similar to those observed in the lighter  $N = 87$  isotones [7–9], in which the collective  $\nu i_{13/2}$  bands terminate at  $I^\pi \sim 41/2^+$  with the oblate configuration and particle-hole excitations dominate the higher-lying level structure. The shape evolution of the  $\nu i_{13/2}$  bands in the  $N = 87$  isotones has been interpreted quite well by the total-energy surface calculation [8]. For these isotones, the Fermi level is positioned near the bottom of the  $i_{13/2}$  sub-shell. Therefore, the  $i_{13/2}$  quasiparticles exert a strong polarizing force that drives the nucleus toward increasing positive  $\gamma$  deformation with increasing angular momentum, and finally reaches the  $\gamma = 60^\circ$  noncollective oblate shape [8]. It should be pointed out that the shape evolution of the  $\nu i_{13/2}$  band in  $^{157}\text{Yb}$  follows generally the systematic of the lighter isotones, but the detailed structure of these  $\nu i_{13/2}$  bands is different; the  $\nu i_{13/2}$  bands in  $^{153}\text{Dy}$  and  $^{155}\text{Er}$  display collective rotational behavior up to the terminating states, while the high-lying part of the  $\nu i_{13/2}$  band in  $^{157}\text{Yb}$  shows a vibration-like structure.

Different excitation modes should be revealed in the plot of  $E_\gamma$  vs. spin  $I$ , here  $E_\gamma$  denoting the energy of  $\gamma$ -ray depopulating the level with a spin value of  $I$ . Ideally, with increasing spin, the transition energies increase linearly for a good rotor and remain constant for a vibrator. Figure 3 displays the  $E_\gamma$ - $I$  plots for the  $\nu i_{13/2}$  bands

in  $^{153}\text{Dy}$ ,  $^{155}\text{Er}$  and  $^{157}\text{Yb}$ . Remarkable features of these plots are that the rotational collectivity of the  $\nu i_{13/2}$  bands both in  $^{153}\text{Dy}$  and  $^{155}\text{Er}$  persists to the  $J = 41/2$  levels at which the bands terminate [7,8], but for the  $\nu i_{13/2}$  band in  $^{157}\text{Yb}$  the transition energies remain constant above the  $I = 25/2$  level. This observation indicates that the shape transition in  $^{157}\text{Yb}$  might take place at lower spins compared to its lighter isotones. The  $Z$ -dependence of the shape transition was also observed in the even-even  $N = 88$  isotones from  $^{154}\text{Dy}$  to  $^{158}\text{Yb}$ , which was nicely interpreted by the cranked modified oscillator calculations of the potential energy surfaces [16]. These calculations show that the potentials become softer with respect to  $\gamma$  vibrations while increasing the proton number in these isotones.

Vibration-like excitations also show up at spins below 18 in the  $N = 86$  isotones [3], and at medium spins from 24 to 36 in the  $N = 88$  nucleus  $^{158}\text{Yb}$  [4]. Baktash *et al.* have investigated these structure systematically [3], and suggested that the vibration-like excitations arise from soft-triaxial to oblate-shape transitions. The cranked shell model calculations indicated that the vibrational excitations are members of rotational bands which continuously minimize their energies by adjusting their shape parameters and acquiring larger  $\gamma$ -values, and finally these bands terminate on the oblate configurations which are formed by the angular-momentum alignments of valence particles along the oblate symmetry axis [5]. However, the interpretation of the vibrational excitations in  $^{158}\text{Yb}$  has been debated [17]. Patel *et al.* suggested that it is the band crossings that caused the vibrational excitations in  $^{158}\text{Yb}$  [17]. As for the  $\nu i_{13/2}$  band in  $^{157}\text{Yb}$ , the BC, EF and  $A_p B_p$  alignments [18–20] may result in deviation of the level energies from the  $E \sim I(I+1)$  relationship. If the energy deviation from rotational pattern was caused by band crossings for the levels above  $I \sim 25/2$  in the  $\nu i_{13/2}$  band of  $^{157}\text{Yb}$ , then the crossing frequencies should be around 0.34 MeV. However, the alignments, which are considered to result in irregular transition energies in narrow band-crossing region, cannot explain the almost constancy of the five consecutive transition energies. Moreover, the above-mentioned alignments occur at higher frequencies in neighboring nuclei [18–20]. Therefore, we conclude preferably that the high-lying part of the  $\nu i_{13/2}$  band in  $^{157}\text{Yb}$  is a consequence of the quasivibrational excitations [4]. Recently, the yrast level structure for the most proton-rich  $N = 87$  nucleus  $^{159}\text{Hf}$  was published [11]. It is surprising that the yrast structure having vibration-like energy spacings is built on the  $\nu h_{9/2}$  configuration. The difference in yrast structure between  $^{159}\text{Hf}$  and the lighter  $N = 87$  isotones is attributed to the lowering of the  $\nu h_{9/2}$  orbital as the number of valence protons increases due to the attractive interaction between the  $\nu h_{9/2}$  and  $\pi h_{11/2}$  configurations [11]. It would be important to search for the excitations in  $^{159}\text{Hf}$  built on the  $\nu i_{13/2}$  configuration, and thus to extend the systematics of the  $\nu i_{13/2}$  bands in the  $N = 87$  isotones.

In summary, the low-lying level scheme of  $^{157}\text{Yb}$  show a co-existence of slightly oblate and weak prolate

deformations. With increasing angular momentum, the  $\nu i_{13/2}$  band in  $^{157}\text{Yb}$  loses gradually its collectivity with its structure evolving into a vibration-like excitations, and finally this band gives way to single-particle excitations. The present work shows the  $N = 87$  nucleus  $^{157}\text{Yb}$  to be transitional in two aspects. Not only does  $^{157}\text{Yb}$  connect the isotopes ( $N < 87$ ) with spherical or oblate shapes to those ( $N > 87$ ) with pronounced prolate shapes, also exhibit structure features of both groups.

The authors wish to thank the staffs of the CIAE tandem accelerator for providing  $^{16}\text{O}$  beam. This work is supported partly by the National Natural Sciences Foundation of China (Grant No. 10005012 and 10025525), the “100 persons project” of the Chinese Academy of Sciences, and the Major State Basic Research Development Program of China (Contract No. G2000077400).

## References

1. A.W. Sunyar, *Phys. Scr.* **24**, 298 (1981).
2. C.J. Lister *et al.*, *Phys. Rev. C* **23**, 2078 (1981).
3. C. Baktash, *Proceedings of the Conference on High Angular Momentum Properties of Nuclei, Oak Ridge, Tennessee, 1982*, edited by N.R. Johnson (1983) p. 207, unpublished.
4. C. Baktash *et al.*, *Phys. Rev. Lett.* **54**, 978 (1985).
5. I. Ragnarsson *et al.*, *Phys. Rev. Lett.* **54**, 982 (1985).
6. P.O. Tjom *et al.*, *Phys. Rev. Lett.* **55**, 2405 (1985).
7. M. Kortelahti *et al.*, *Phys. Lett. B* **131**, 305 (1983).
8. F.A. Beck *et al.*, *Phys. Lett. B* **192**, 49 (1987).
9. N. Nica *et al.*, *Phys. Rev. C* **64**, 034313-1 (2001).
10. P. Kleinheinz *et al.*, *Nucl. Phys. A* **283**, 189 (1977).
11. K.Y. Ding *et al.*, *Phys. Rev. C* **62**, 034316-1 (2000).
12. D. Horn *et al.*, *Bull. Am. Phys. Soc.* **24**, 694 (1979).
13. A. Hashizume *et al.*, *RIKEN Accel. Progr. Rep.*, **16**, 41 (1983).
14. M.H. Rafailovich *et al.*, *Phys. Rev. C* **30**, 169 (1984).
15. M. Sugawara *et al.*, *Nucl. Phys. A* **686**, 29 (2001).
16. S. Aberg, *Phys. Scr.* **25**, 113 (1982).
17. S.B. Patel *et al.*, *Phys. Rev. Lett.* **57**, 62 (1986).
18. L.L. Riedinger, *Nucl. Phys. A* **347**, 141 (1980).
19. M.A. Riley *et al.*, *Phys. Lett. B* **135**, 275(1984).
20. T. Byrski, *Phys. Lett. B* **102**, 235 (1981).